

Quantitative analysis of retinal vasculature in normal eyes using ultra-widefield fluorescein angiography

Jing-Wen Jiang, Zuo-Hui-Zi Yi, Xiao-Ling Wang, Jue-Jun Liu, Gong-Peng Sun, Chang-Zheng Chen

Eye Center, Renmin Hospital of Wuhan University, Wuhan 430060, Hubei Province, China

Correspondence to: Chang-Zheng Chen. Renmin Hospital of Wuhan University, No.9 ZhangZhiDong Street, Wuchang District, Wuhan 430060, Hubei Province, China. whuchenchzh@163.com

Received: 2021-03-21 Accepted: 2021-08-26

Abstract

● **AIM:** To quantify the area and density of retinal vascularity by ultra-widefield fluorescein angiography (UWFA).

● **METHODS:** In a retrospective study, UWFA images were obtained using an ultra-widefield imaging device in 42 normal eyes of 42 patients. Central and peripheral steered images were used to define the edge of retinal vasculature by a certified grader. The length from the center of the optic disc to the edge of retinal vascularity (RVL) in each quadrant and the total retinal vascular perfusion area (RVPA) were determined by the grader using OptosAdvance software. The density of retinal vascularity (RVD) was quantified in different zones of central-steered images using Image J software.

● **RESULTS:** Among 42 healthy eyes, the values for mean RVL in each quadrant were 19.007±0.781 mm (superior), 18.467±0.869 mm (inferior), 17.738±0.622 mm (nasal) and 24.241±1.336 mm (temporal). The mean RVPA was 1140.117±73.825 mm². The mean RVD of the total retina was 4.850%±0.638%. RVD varied significantly between different retina zones ($P<0.001$), and significant differences existed in the RVD values for total retinal area in patients over 50 years old compared to those under 50 years old ($P=0.033$). No gender difference was found.

● **CONCLUSION:** The UWFA device can be a promising tool for analyzing the overall retinal vasculature and may provide a better understanding of retinal vascular morphology in normal eyes. Aging may be related to lower RVD.

● **KEYWORDS:** ultra-widefield fluorescein angiography; retinal; vasculature; imaging

DOI:10.18240/ijo.2021.12.16

Citation: Jiang JW, Yi ZHZ, Wang XL, Liu JJ, Sun GP, Chen CZ. Quantitative analysis of retinal vasculature in normal eyes using ultra-widefield fluorescein angiography. *Int J Ophthalmol* 2021;14(12):1915-1920

INTRODUCTION

The ultra-widefield fluorescein (UWFA) system provides 200° visual coverage of the retina area, covering more than 80% of the retinal surface in a single image, and can image significantly larger retinal areas compared to conventional 7-field montaged image^[1-2]. With the UWFA system, retinal images can be acquired at the same time point after the injection of fluorescein without montage processing, therefore providing a more accurate depiction of the retinal perfusion situation. UWFA has become a useful tool in clinical practice, as it is conducive to the diagnosis, treatment and follow-up tracing of multiple retinal diseases^[3-7].

Studies have revealed that peripheral retinal nonperfusion closely correlated, in terms of both severity and activity, to the presence of retinal vascular diseases such as retinal vein occlusion (RVO) and diabetic retinopathy (DR)^[3-7]. Thus, evaluating the precise area of retinal nonperfusion has particularly vital value in the diagnosis and management of retinal vascular diseases. Recently, ischemic index (ISI, nonperfused area/gradable retina) obtained from UWFA images has been shown to be associated with macular edema and neovascularization in RVO and DR patients^[6-10]. Furthermore, several studies have observed the presence of periphery retinal capillary nonperfusion in healthy eyes^[11], suggesting that periphery retinal nonperfusion may be physiological. Therefore, improved quantification of retinal vasculature in healthy eyes, and a better understanding of the vasculature features, would provide important clinical benefits. The projection from three-dimensions to two-dimensions causes nonnegligible peripheral distortions in UWFA images^[12-13], generating a potential difference in the actual peripheral retinal data and data obtained from UWFA images. California (Optos, Dunfermline, Scotland, UK) is a late-model of Optos ultra-widefield imaging devices. The distortions at the image periphery can be corrected on California, providing

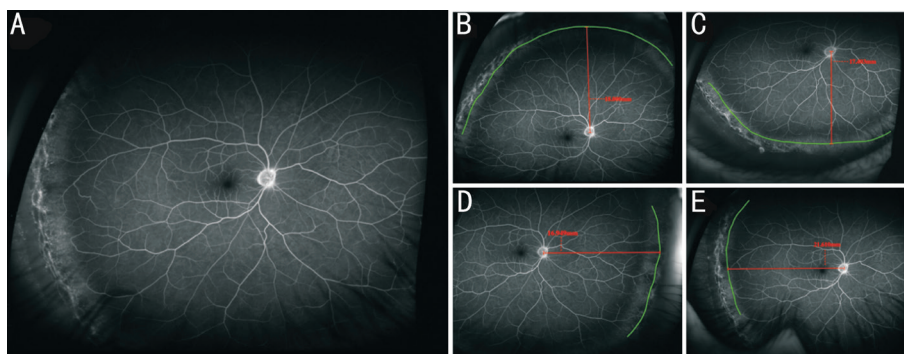


Figure 1 Assessment of the distances from center of optic disk to edges of retinal vasculature of UWFA images in a normal eye A: The central-steered UWFA image; B-E: Peripheral-steered (superior, inferior, nasal, temporal) UWFA images in the same eye. The edges of retinal vasculature were manually outlined (green line) and distances from optic disk to it were measured (red line). The measured data were 18.000 mm, 17.403 mm, 16.949 mm and 21.610 mm respectively.

a display that is more similar to the actual retina^[14]. Moreover, OptosAdvance software on California can be used to measure precise distance in millimeters (mm) or area in mm^2 instead of pixels or disc areas. Therefore, the California system has the potential to be the ideal tool for quantifying the overall retinal vasculature.

We sought to quantify the retinal vasculature with central and peripheral fixation UWFA images in healthy eyes using the California system. Measurements included retinal vascular perfusion bed (RVPA) in mm^2 , lengths from the center of optic disk to the edges of retinal vasculature (RVL) in each quadrant in mm, and density of retinal vasculature (RVD, %). We also divided RVD into 4 different zones (peri-macular, near-peripheral, mid-peripheral and total-retinal) using the concentric ring method^[15] in order to identify possible differences.

SUBJECTS AND METHODS

Ethical Approval This study adhered to the tenets of the Declaration of Helsinki and was approved by the Ethics Committee of Renmin Hospital of Wuhan University (approved No. WDRY2019-K037). The informed consents were obtained from all participants.

Subjects In this retrospective study, 42 eyes from 42 patients in Renmin Hospital of Wuhan University from June 2019 to August 2019 were analyzed. These patients originally underwent UWFA examination (Optos California ultra-widefield imaging device; Dunfermline, Scotland, UK), including central and four position steering, due to the presence of central serous chorioretinopathy, low to moderate myopia or mild cataract, or subjective visual disturbances. Patients whose eyes displayed a known or potential disease, especially RVO, uveitis, glaucoma and pathologic myopia, or patients with a history of vitreoretinal surgery, were excluded. Patients with diabetes, hypertension, or other systemic diseases that could affect retinal circulation, as well as patients under 18 years old or over 80 years old, were excluded.

Acquisition of Images The UWFA images of 42 eyes were reviewed for clarity and quality on Optos California. For each eye, images in the early (0-45s), mid (45s to 2min), and late (5-10min) phases of fluorescein angiography were obtained, as well as mid phase images in four steering positions (superior, inferior, nasal, temporal).

Assessment of Images All images were graded by an experienced ophthalmologist. The edges of retinal vasculature were manually outlined in images obtained from the four steering positions of each eye, and RVL was measured using OptosAdvance software by the grader (Figure 1). In each peripheral-steered image, part of the area was measured manually according to the shape of retinal vasculature and RVPA was calculated as the sum of the measured values.

Central-steered UWFA images were manually divided by the grader into 3 concentric zones using OptosAdvance software. The center of the concentric ring was the macula fovea, and areas within a radius of 3 mm, 10 mm and 15 mm were defined as peri-macular area (PMA), near-peripheral area (NPA) and mid-peripheral area (MPA), respectively, and are denoted as zones 1-3. The binarization of UWFA images was performed using Image J software version 2.0.0 (US National Institutes of Health, Bethesda, Maryland USA). Central-steered UWFA images were imported into ImageJ and converted to 8-bit. Using a morphological filter and threshold method, the 8-bit images were binarized to black and white pixels, with areas of vasculature shown in white. Graders manually outlined and segmented the region of the total gradable retinal area according to the original UWFA images. RVD was automatically calculated by the software as the proportion of white area in zones 1-3 compared to the total gradable retinal area (Figures 2 and 3).

Statistical Analysis Statistical analyses were performed using SPSS statistical software version 23.0 (SPSS Inc, IBM, Chicago, IL, USA). Independent *t*-tests were used to analyze

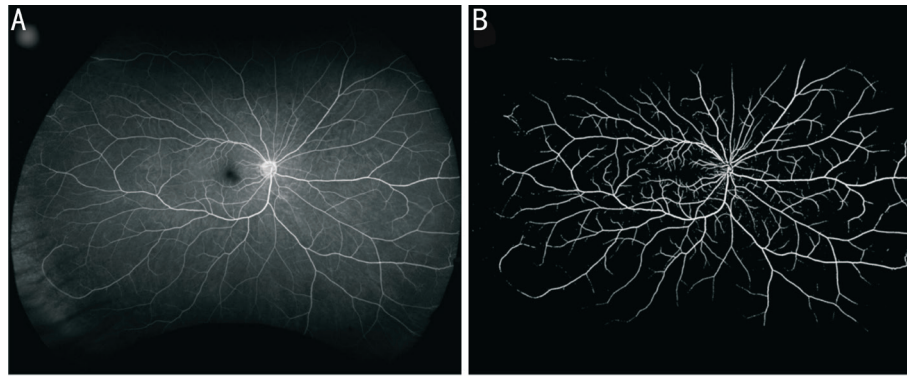


Figure 2 Binarization and zone partition of UWFA image in a normal eye A: A central-steered UWFA image; B: The resulting image after binarization.

RVL, RVPA and RVD from different genders. The values of RVD from different zones were analyzed using Kruskal-Wallis and Bonferroni tests. Patients were divided into 2 groups according to age (group 1: <50y, group 2: ≥50y) and Mann-Whitney *U* tests were used to analyze RVL and RVD from different age groups. $P < 0.05$ was considered statistically significant.

RESULTS

Descriptive Characteristics of Demography and Retinal Vasculature In this group, all 42 patients were Chinese and 27 (64.3%) were male. The mean age was 49y (range 18-72y). Of the 42 normal eyes, 24 right eyes (57.1%) and 18 left eyes (42.9%) were included. The mean RVL was 19.007 ± 0.781 mm in the superior area, 18.467 ± 0.869 mm in the inferior area, 17.738 ± 0.622 mm in the nasal area and 24.241 ± 1.336 mm in the temporal area. The mean RVPA was 1140.117 ± 73.825 mm². The mean RVD of the total retinal area was $4.850\% \pm 0.638\%$.

Quantitative Analysis of RVL, RVPA, and RVD from Different Genders Results of the independent *t*-tests showed that in each quadrant, there was no significant difference in mean RVL from different genders (superior: $t=0.934$, $P=0.356$; inferior: $t=-1.529$, $P=0.134$; nasal: $t=-1.757$, $P=0.087$; temporal: $t=-0.432$, $P=0.668$). Similarly, there was no significant difference in RVPA and RVD between different genders (RVPA: $t=-0.031$, $P=0.976$; RVD: $t=-0.578$, $P=0.561$).

Quantitative Analysis of RVD from Different Retinal Zones The mean RVD values from different zones were $9.240\% \pm 1.668\%$ (zone 1), $9.394\% \pm 1.103\%$ (zone 2), $6.050\% \pm 0.748\%$ (zone 3) and $4.850\% \pm 0.638\%$ (total area). Kruskal-Wallis tests showed differences in the RVD of different retinal zones ($H=130.982$, $P < 0.001$). After correcting the significance level using Bonferroni tests, significant differences were found between zone 3 and zones 1-2, and the total area and zones 1-3 (all $P < 0.001$; Figure 4).

Quantitative Analysis of RVD and RVL from Different Age Groups Although the mean RVD in each region was slightly

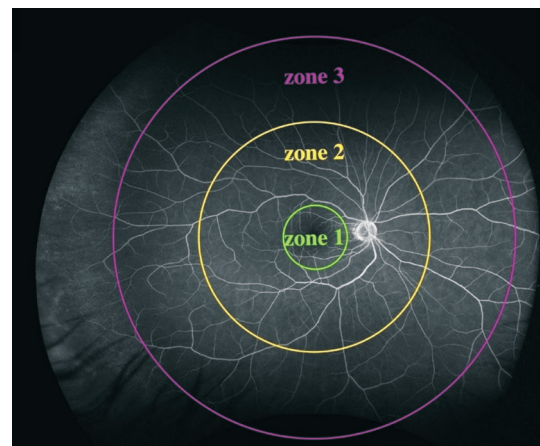


Figure 3 UWFA image was manually divided into 3 concentric-ring zones (green circle for zone 1, yellow circle for zone 2, purple circle for zone 3) using OptosAdvance software.

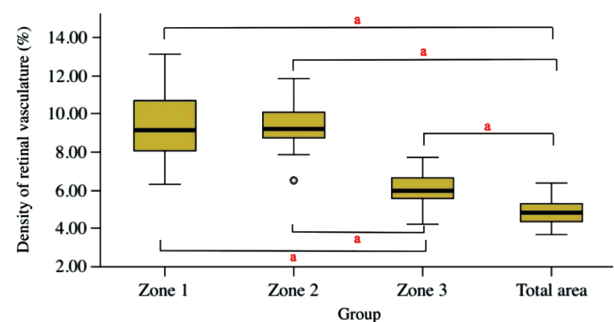


Figure 4 Zone 1-zone 3 represented PMA, NPA and MPA respectively Kruskal-Wallis test for density of retinal vasculature (RVD) from different zones and RVD from each two zones were compared using Bonferroni test. ^a $P < 0.001$.

lower in patients above 50 years old (age group 2) than that in younger patients (age group 1), no statistical difference could be detected between the age groups in zone 1-3 ($P=0.115$, 0.178 , 0.071 respectively, Mann-Whitney *U* test). However, for total retinal area, RVD in patients over 50y was significantly lower than in patients under 50y ($P=0.033$, Mann-Whitney *U* test; Table 1). No statistically significant difference was found between the two age groups for the mean RVL values obtained

for the superior, inferior, nasal and temporal quadrants ($P=0.115, 0.213, 0.067$ and 0.416 respectively, Mann-Whitney U test; Table 2).

DISCUSSION

The development of the UWFA system not only allows for a 200° field of vision, but also provides a new quantification mode which will help further clinical research on fundus. This method has been widely used in previous studies, particularly those analyzing ISI, as this method is helpful for clinical diagnosis, treatment, and follow-up. In order to accurately describe the degree of pathological retinal nonperfusion, the physiologic nonperfusion area should be excluded from the total visible retina when calculating ISI, and the normal peripheral retinal anatomy should be used as the reference standard when analyzing pathological UWFA retinal vasculature^[11]. Therefore, it is essential to understand the normal peripheral vascular system of the retina, and our study may shed some light on this.

The results of our previous study have observed vascular anastomosis with a peripheral avascular area in 36.23% eyes in normal eyes^[16]. Therefore, it's essential to investigate the perfusion area of retinal vascularity in normal eyes. As mentioned above, earlier systems such as the Optos 200tx were hindered by the peripheral distortion caused by the transformation of a 3D image into a 2D image, however this has been overcome in newest UWFA device, Optos California. To our knowledge, our study is the first to perform quantitative analysis of retinal vasculature in healthy eyes using the California system. Similar studies have been performed by the Sadda lab to quantify the retinal vasculature in 59 normal eyes using the 200tx device^[17-18], and while the outcomes of our studies showed some similarities, there were still some important differences. The most apparent difference was in the values obtained for RVP. Our study suggested a significantly larger value of the mean RVP (1140.1 mm² vs 977.0 mm²), whereas the differences in the RVL in each quadrant (superior: 19.0 mm vs 19.2 mm, inferior: 18.5 mm vs 20.4 mm, nasal: 17.7 mm vs 17.4 mm, temporal: 24.2 mm vs 22.5 mm) or RVD of the total retina (4.8 % vs 4.3 %) were relatively similar. Possible reasons for the differences could be the different devices, populations or image processing methods, and large sample studies may be needed to provide more comprehensive results.

When performing the image processing for RVD, we referred to a previous study by Wang *et al*^[16] which used the concentric-ring method to divide the retina. Our results suggest that the distribution of retinal vasculature in the periphery was significantly lower than in the central area. Correspondingly, the photoreceptors in the retina have similar regional characteristics. The cone cell density in the central fovea is

Table 1 Retinal vascular density in different regions from different age groups

Region	RVD from different age groups (%)		P
	Group 1: <50y (n=18)	Group 2: ≥50y (n=24)	
Zone 1	9.709±1.497	8.887±1.733	0.115
Zone 2	9.679±1.056	9.180±1.110	0.178
Zone 3	6.293±0.672	5.868±0.763	0.071
Total area	5.103±0.627	4.660±0.589	0.033 ^a

RVD: Retinal vascular density. ^a $P<0.05$; Mann-Whitney U test.

Table 2 Length from the optic disc to the edge of retinal vascularity in different quadrants in different age groups

Quadrant	RVL from different age group (mm)		P
	Group 1: <50y (n=18)	Group 2: ≥50y (n=24)	
Superior	19.220±0.812	18.848±0.640	0.115
Inferior	18.651±0.894	18.328±0.842	0.213
Nasal	17.970±0.512	17.564±0.650	0.067
Temporal	24.437±1.381	24.094±1.311	0.416

RVL: Length from center of optic disc to edge of retinal vascularity. Mann-Whitney U test.

extremely high, where there is a 100-200 μm rod-free zone, then the density of cone cells drops sharply from the central fovea to the periphery, while the rod cells increase rapidly from the central fovea to the periphery, where they reach their highest density at 3-5 mm^[19]. Photoreceptors consume significant amounts of energy and oxygen; hence their energy metabolism is closely related to vision^[20]. Nonperfusion in the area with high photoreceptor density leads to increased production of vascular endothelial growth factor (VEGF), which can cause more severe neovascularization and macular edema. Previous studies have found that in eyes with RVO and PDR, the ISI value increased from posterior pole to periphery, and a larger ISI value in the peripheral retina could be associated with a worse visual outcome^[1,8]. Therefore, the results of our study on the distribution of retinal vessels in different regions may be useful for further study on the differences in ISI of the affected eyes and could help determine whether different treatment strategies should be adopted for different retinal areas.

Whether aging is related to retinal vascular perfusion has always been an area of intense interest for researchers. The outcome of our study showed that the RVD of total visible retinal area on UWFA could evidently decrease in elder patients over 50y. Interestingly, a recent study showed that retinal arterioles were thinner in patients with hypertension in ultra-widefield fundus imaging^[21]. Similar to the vascular change in patients with hypertension, studies have shown that with the increase of age, the artery of normal people is

also diffusely calcified, and its diameter becomes thinner^[22]. Therefore, we speculate that people over 50 years old are more likely to have atherosclerosis changes similar to those with hypertension, resulting in decreased retinal RVD. Along with the changes of retinal arterioles, using optical coherence tomography angiography (OCTA), former studies have proposed that the vascular system of the retina in healthy eyes would decrease in density and reduce blood flow velocity in microvasculature in the process of aging, which may be caused by the degeneration of nervous system or cerebral vascular system during normal aging^[23-24]. However, OCTA can only provide vascular morphology information for the posterior pole, and there have been few studies on the relationship between aging and total retina vascular density. Wide-field swept-source optical coherence tomography angiography (WF-SSOCTA) provides technical advances as well as a high-definition view of 70°-80° of the retina in a merged image^[25]. Compared with UWFA, WF-SSOCTA offers superior detail display and is not affected by fluorescein leakage. In addition, WF-SSOCTA has been shown to produce reproducible results when analyzing capillary anatomy^[25]. Combinatorial use of UWFA and WF-SSOCTA could be promising for future studies and may allow for more reliable quantitative analysis of possible changes in retinal vessels in normal eyes that occur during the aging process. Interestingly, previous studies have revealed that choroidal thickness (CT) decreases with increasing age^[26-27], indicating that besides the changes of RVD observed in this study, choroidal vascular perfusion may also be affected by age, while similarities and differences between retinal and choroidal perfusion responses to age changes still needs further research. Furthermore, our study found no statistical difference between RVL and age in each quadrant, which is contrary to results from previous studies^[17-18]. Therefore, whether retinal perfusion distance could be affected by aging still requires further large-scale analysis.

Our results were obtained from a retrospective study with a limited number of samples, and we only used a rough age stratification, both of which imposed potential limitations on our analysis. Furthermore, healthy samples were rare due to ethical issues, so unfortunately, some of the participants did not show full binocular health. Thus, prospective studies with a larger sample of fully healthy participants may be needed in the future. In addition, because of the influence of background fluorescein and the eyelash occlusion artifact, our binarization result was inevitably different from the real fundus. Although the California system has corrected the peripheral distortion, there may still remain an unavoidable error in the measurement value in peripheral image.

In conclusion, UWFA device enables the visualization and quantification of retinal vasculature, and this new method

may reveal important information regarding retinal vascular morphology in normal eyes. Our results provided a basis for analyzing physiological retinal vascular perfusion and showed that aging may be related to lower density of retinal vascularity, but further analysis is required.

ACKNOWLEDGEMENTS

Conflicts of Interest: Jiang JW, None; Yi ZHZ, None; Wang XL, None; Liu JJ, None; Sun GP, None; Chen CZ, None.

REFERENCES

- 1 Kang W, Ghasemi Falavarjani K, Nittala MG, Min SG, Wykoff CC, van Hemert J, Ip M, Sadda SR. Ultra-wide-field fluorescein angiography-guided normalization of ischemic index calculation in eyes with retinal vein occlusion. *Invest Ophthalmol Vis Sci* 2018;59(8):3278-3285.
- 2 Patel M, Kiss S. Ultra-wide-field fluorescein angiography in retinal disease. *Curr Opin Ophthalmol* 2014;25(3):213-220.
- 3 Torp TL, Kawasaki R, Wong TY, Peto T, Grauslund J. Peripheral capillary non-perfusion in treatment-naïve proliferative diabetic retinopathy associates with postoperative disease activity 6mo after panretinal photocoagulation. *Br J Ophthalmol* 2019;103(6):816-820.
- 4 Prasad PS, Oliver SC, Coffee RE, Hubschman JP, Schwartz SD. Ultra wide-field angiographic characteristics of branch retinal and hemicentral retinal vein occlusion. *Ophthalmology* 2010;117(4):780-784.
- 5 Singer M, Tan CS, Bell D, Sadda SR. Area of peripheral retinal nonperfusion and treatment response in branch and central retinal vein occlusion. *Retina* 2014;34(9):1736-1742.
- 6 Tsui I, Kaines A, Havunjian MA, Hubschman S, Heilweil G, Prasad PS, Oliver SC, Yu F, Bitrian E, Hubschman JP, Friberg T, Schwartz SD. Ischemic index and neovascularization in central retinal vein occlusion. *Retina* 2011;31(1):105-110.
- 7 Wessel MM, Nair N, Aaker GD, Ehrlich JR, D'Amico DJ, Kiss S. Peripheral retinal ischaemia, as evaluated by ultra-widefield fluorescein angiography, is associated with diabetic macular oedema. *Br J Ophthalmol* 2012;96(5):694-698.
- 8 Fan WY, Nittala MG, Velaga SB, Hirano T, Wykoff CC, Ip M, Lampen SIR, van Hemert J, Fleming A, Verhoek M, Sadda SR. Distribution of nonperfusion and neovascularization on ultrawide-field fluorescein angiography in proliferative diabetic retinopathy (RECOVERY study):report 1. *Am J Ophthalmol* 2019;206:154-160.
- 9 Thomas AS, Thomas MK, Finn AP, Fekrat S. Use of the ischemic index on widefield fluorescein angiography to characterize a central retinal vein occlusion as ischemic or nonischemic. *Retina* 2019;39(6):1033-1038.
- 10 Tan CS, Chew MC, van Hemert J, Singer MA, Bell D, Sadda SR. Measuring the precise area of peripheral retinal non-perfusion using ultra-widefield imaging and its correlation with the ischaemic index. *Br J Ophthalmol* 2016;100(2):235-239.
- 11 Shah AR, Abbey AM, Yonekawa Y, Khandan S, Wolfe JD, Trese MT, Williams GA, Capone A Jr. Widefield fluorescein angiography in patients without peripheral disease: a study of normal peripheral findings. *Retina* 2016;36(6):1087-1092.

- 12 Nicholson L, Goh LY, Marshall E, Vazquez-Alfageme C, Chatziralli I, Clemo M, Hykin PG, Sivaprasad S. Posterior segment distortion in ultra-widefield imaging compared to conventional modalities. *Ophthalmic Surg Lasers Imaging Retina* 2016;47(7):644-651.
- 13 Oishi A, Hidaka J, Yoshimura N. Quantification of the image obtained with a wide-field scanning ophthalmoscope. *Invest Ophthalmol Vis Sci* 2014;55(4):2424-2431.
- 14 Kato Y, Inoue M, Hirakata A. Quantitative comparisons of ultra-widefield images of model eye obtained with Optos® 200Tx and Optos® California. *BMC Ophthalmol* 2019;19(1):115.
- 15 Nicholson L, Vazquez-Alfageme C, Ramu J, Triantafyllopoulou I, Patrao NV, Muwas M, Islam F, Hykin PG, Sivaprasad S. Validation of concentric rings method as a topographic measure of retinal nonperfusion in ultra-widefield fluorescein angiography. *Am J Ophthalmol* 2015;160(6):1217-1225.e2.
- 16 Wang XL, Xu A, Yi Z, He L, Liu JJ, Zheng HM, Chen CZ. Observation of the far peripheral retina of normal eyes by ultra-wide field fluorescein angiography. *Eur J Ophthalmol* 2021;31(3):1177-1184.
- 17 Singer M, Min SG, van Hemert J, Kuehlewein L, Bell D, Sadda SR. Ultra-widefield imaging of the peripheral retinal vasculature in normal subjects. *Ophthalmology* 2016;123(5):1053-1059.
- 18 Fan WY, Uji A, Borrelli E, Singer M, Sagong SG, van Hemert J, Sadda SR. Precise measurement of retinal vascular bed area and density on ultra-wide fluorescein angiography in normal subjects. *Am J Ophthalmol* 2018;188:155-163.
- 19 Curcio CA, Sloan KR, Kalina RE, Hendrickson AE. Human photoreceptor topography. *J Comp Neurol* 1990;292(4):497-523.
- 20 Narayan DS, Chidlow G, Wood JP, Casson RJ. Glucose metabolism in mammalian photoreceptor inner and outer segments. *Clin Exp Ophthalmol* 2017;45(7):730-741.
- 21 Robertson G, Fleming A, Williams MC, Trucco E, Quinn N, Hogg R, McKay GJ, Kee F, Young I, Pellegrini E, Newby DE, van Beek EJR, Peto T, Dhillon B, van Hemert J, MacGillivray TJ, Northern Ireland Cohort of Longitudinal Ageing. Association between hypertension and retinal vascular features in ultra-widefield fundus imaging. *Open Heart* 2020;7(1):e001124.
- 22 Tesauro M, Mauriello A, Rovella V, Annicchiarico-Petruzzelli M, Cardillo C, Melino G, Di Daniele N. Arterial ageing: from endothelial dysfunction to vascular calcification. *J Intern Med* 2017;281(5):471-482.
- 23 Wei YT, Jiang H, Shi YY, Qu DY, Gregori G, Zheng F, Rundek T, Wang JH. Age-related alterations in the retinal microvasculature, microcirculation, and microstructure. *Invest Ophthalmol Vis Sci* 2017;58(9):3804-3817.
- 24 Lin Y, Jiang H, Liu Y, Rosa Gameiro G, Gregori G, Dong CH, Rundek T, Wang JH. Age-related alterations in retinal tissue perfusion and volumetric vessel density. *Invest Ophthalmol Vis Sci* 2019;60(2):685-693.
- 25 Eastline M, Munk MR, Wolf S, Schaal KB, Ebnetter A, Tian M, Giannakaki-Zimmermann H, Zinkernagel MS. Repeatability of wide-field optical coherence tomography angiography in normal retina. *Transl Vis Sci Technol* 2019;8(3):6.
- 26 Ruiz-Medrano J, Ruiz-Moreno JM, Goud A, Vupparaboina KK, Jana S, Chhablani J. Age-related changes in choroidal vascular density of healthy subjects based on image binarization of swept-source optical coherence tomography. *Retina* 2018;38(3):508-515.
- 27 Zhou H, Dai YN, Shi YY, Russell JF, Lyu CC, Noorikolouri J, Feuer WJ, Chu ZD, Zhang QQ, de Sisternes L, Durbin MK, Gregori G, Rosenfeld PJ, Wang RK. Age-related changes in choroidal thickness and the volume of vessels and stroma using swept-source OCT and fully automated algorithms. *Ophthalmol Retina* 2020;4(2):204-215.